Title

Feature Extraction and NN-Based Enhanced Test Maneuver Deployment for 2 DoF Vehicle Simulator

Authors

Demir, Uğur

Akgün, Gazi

Aküner, Mustafa Caner

et al.

Publication Date

2023

DOI

10.1109/access.2023.3266326

IEEE Access
Multidisciplinary | Rapid Review | Open Access Journal

Received 26 March 2023, accepted 6 April 2023, date of publication 11 April 2023, date of current version 14 April 2023.

Digital Object Identifier 10.1109/ACCESS.2023.3266326

RESEARCH ARTICLE

Feature Extraction and NN-Based Enhanced Test Maneuver Deployment for 2 DoF Vehicle Simulator

UĞUR DEMİR[1,2], GAZİ AKGÜN[1], MUSTAFA CANER AKÜNER[1], BORA DEMİRCİ[1], OMER AKGUN[3], AND TAHIR CETIN AKINCI[4,5], (Senior Member, IEEE)

[1]Department of Mechatronics Engineering, Marmara University, 34852 Istanbul, Turkey
[2]Department of Electrical and Computer Engineering, Texas A&M University, College Station, TX 77843, USA
[3]Department of Computer Engineering, Marmara University, 34852 Istanbul, Turkey
[4]Department of Electrical Engineering, Istanbul Technical University, 34469 Istanbul, Turkey
[5]WCGEC, University of California at Riverside, Riverside, CA 92507, USA

Corresponding author: Tahir Cetin Akinci (tahircetin.akinci@ucr.edu)

This work was supported by the Marmara University Scientific Research Projects Commission under Project FYL-2022-10537.

ABSTRACT This paper presents a deployment method of various test maneuver scenarios for 2 degree of freedom (2 DoF) vehicle simulator by using feature extraction and neural networks (NN). A prototype version has been set up for the 2 DoF vehicle simulator. Then, a hardware in the loop (HIL) model with 2 inputs (torque, τ_1- τ_2) and 3 outputs (acceleration, a_x-a_y-a_z) is created. System identification is performed to obtain the training data of NNs to be used for the deployment of test maneuvers. In the system identification process, 2 arbitrary sinusoidal torque signals (τ_1- τ_2) are generated by using the actuator specs of the 2 DoF vehicle simulator. By applying the generated torque signals to the actuators, acceleration (a_x-a_y-a_z) data are collected from the inertial measurement sensor (IMU) on the 2 DoF vehicle simulator. It is determined to create 3 different NN models for the obtained data. The 1st NN model is trained with 3 inputs (a_x-a_y-a_z) and 2 targets (τ_1- τ_2) training data. The 2nd NN model is trained with 6 inputs (amplitudes and phases of a_x-a_y-a_z) and 2 targets (τ_1- τ_2) training data. The input data features for the 2nd NN model is extracted by using the Fast Fourier Transform (FFT). The 3rd NN model is trained with 6 inputs (amplitudes and phases of a_x-a_y-a_z) and 4 targets (amplitudes and phases of τ_1- τ_2) training data. For the 3rd NN model, the features of input and target data are extracted by using the FFT. The NN training process continues until acceptable performance criteria are reached. Then, 3 NN models are run and analysed under various test scenarios such as Double Lane Change, Constant Radius, Increase Steer, Fish Hook, Sine with Dwell and Swept Sine. Only for the 3rd NN, the actuator signals (τ_1- τ_2) are recomposed by applying an inverse FFT process to the 4 targets (amplitudes and phases of τ_1- τ_2). Finally, the reference trajectory tracking performances are evaluated by comparing the NN models that are run under the test scenarios.

INDEX TERMS Feature extraction, IoT, neural networks, system identification, vehicle simulator.

I. INTRODUCTION

The vehicle simulators are mechatronic systems designed to replicate the experience of driving a real vehicle under various driving scenarios or cycles [1]. They are commonly used for purposes such as driver training and games. Simulators allow for the realistic transfer of driving sensations to the driver, enabling measurement of their reactions and evaluation of their performance [2]. Vehicle simulators typically utilize a parallel manipulator structure, such as the Stewart platform shown in Fig. 1 [3].

The orientation of the platforms is changed through sequential movements of linear actuators, with feedback signals generated to keep the platform in the desired orientation, including displacement, velocity, and acceleration information [4], [5]. Realistic driving sensations are achieved by

The associate editor coordinating the review of this manuscript and approving it for publication was Yen-Lin Chen.

transferring the reference accelerations of the linear actuators, fed with real driving information from the mobile platform on which the driver sits, to the mobile platform itself. The degree of freedom (DoF) over the connection points of the mobile platform and the number of actuators used can vary depending on the desired simulation [6]. However, transferring accelerations in the *x*-*y*-*z* axes through different structural connections, along with varying numbers of actuators, can result in nonlinear controller requirements [7]. To address this, neural network-based controller structures have been developed for nonlinear problems, and have gained popularity in the literature [8].

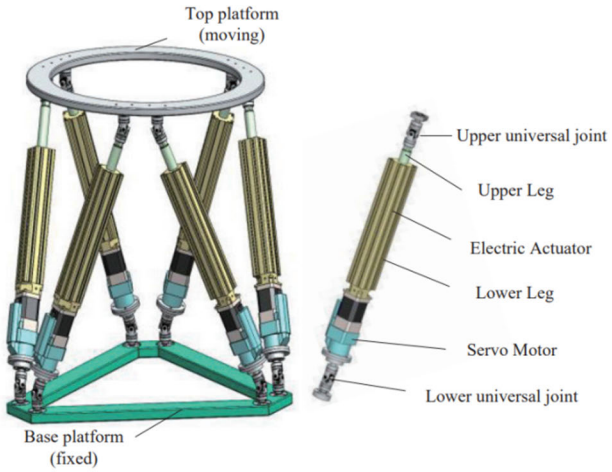

FIGURE 1. Stewart platform [3].

Neural networks have proven to be powerful tools for solving nonlinear problems, offering capabilities such as parameter fitting, classification, and estimation [9], [10], [11], [12], [13]. By using a neural network approach to generate reference signals for linear actuators based on acceleration data in the *x*-*y*-*z* axes obtained from real driving scenarios, a realistic driving experience can be created for the driver on a vehicle simulator. It is of great importance to deploy the data to the vehicle simulator with minimum loss in order to create the real driving feeling. Therefore, the Internet of Things (IoT) has the potential to greatly facilitate the transfer and processing of data in this context. With the aid of servers over the internet, high processing power can be harnessed to analyse signals from sub-actuator and sensor units connected to a central processor, and to generate the necessary control signals for the vehicle simulator [14].

There are many studies on simulators in the literature. These are studied on various software and hardware platforms for air, sea and land vehicles. Since the main subject of this study is a hardware-based simulator platform, hardware-based simulator studies as a result of literature review have been tried to be summarized as follows.

Simulator structures, which usually contain low-cost parallel manipulators, are used within the scope of hardware in the loop (HIL) [5]. Torque control algorithms of hybrid electric vehicles of serial and parallel powertrain configurations on simulators were tried to be evaluated within the scope of human powered vehicles [15]. Similarly, the evaluation of the drowsy driver's lack of reaction during collision detection and action was performed in the vehicle simulator [16]. Evaluation of realistic responses and simulator skills on a hexapod platform and improvement with washout filter were carried out [17]. In another study, it describes the improvement of the Human in the loop powertrain design by analysing it with Unity-Matlab-Simulink© and Driving Cycle in order to increase the performance and range of electric vehicles [18]. The effects of neuromuscular dynamics on steering ability were investigated, in which the behavioural tendency of the driver was analysed both in the real environment and on the simulator platform [19]. For train driver training, 3 DoF (degree of freedom) dynamic simulator was studied. Driving training is carried out under a structure in which the platform is controlled with motion cueing [20]. How an autonomous vehicle is affected by a real driver in order to change lanes safely is analyses. By investigating the parameters of relative distance and relative speed, it has been observed that relative distance plays an important role for a more comfortable driving [21]. With the scenario in the loop, the safety performance of autonomous vehicles was tested with digital twin and unity and tried to be verified with the real vehicle. Vehicle behaviour is tried to be improved with realistic traffic scenarios [22]. Error minimization was studied with adaptive linear quadratic regulated motion cueing algorithm (MCA) in order to create a realistic driving feeling on 8 DoF driving simulators [23]. It has been studied to improve the technical arguments by using genetic algorithm for the optimization of 3 different motion systems on 7 DoF vehicle simulators [24]. Sliding mode control and model predictive control were studied on how to drive the motion cueing algorithm (MCA) to the system on the 4 DoF driving platform. Evaluations were made on pitch, roll, sway, and surge, and it was observed that the sliding mode control has a saturation function and the model predictive controller (MPC) gave better results [25]. Due to the high financial requirements of high-fidelity driving simulator within the scope of human machine interaction, a platform was studied on a medium-fidelity flexible and reusable platform that can provide testing of automotive components by increasing the flexibility of existing systems [26]. An algorithm that can detect the posture of the driver on the motorcycle and correct the posture with various maneuvers while driving is studied [27]. Optimization with nonlinear scaling and genetic algorithm was studied to create a more realistic driving feeling by working on the MPC-based MCA algorithm [28]. The mechanical design and control of the 6 DoF driving platform was studied. Lateral and longitudinal directives are used to give acceleration and motion cues (MC) [29]. With a HIL-based simulator, the development of the driveline was studied by examining the anti-windup effects on the driveline in different ground scenarios in

off road conditions [30]. Motion cueing was studied on a 2-link driving simulator with 3 DoF and innovative structure [31]. MPC based MCA and Classical Washout-based MCA (CW-MCA) were handled comparatively and the control signals needed for real driving feeling were tried to be derived by NN-MCA by working on Neural network-based MCA (NN-MCA) [32]. Comparative analysis between a scaled test vehicle and a software-based full-scale vehicle model was performed. Longitudinal and lateral controllers were designed and their effects on vehicle dynamics were investigated [33]. The electric powered assisted steering system for 3 DoF vehicle models was tried to be analysed within the scope of human driver interaction in terms of crosswind effect [34]. Within the scope of human machine interaction, a driving simulator was studied in order to investigate the pedestrian collision situations, which are frequently experienced during right turns, in 5 steps [35]. Yaw moment control algorithm was tried to be developed by using Buckingham II theory on a scaled vehicle [36]. A simulator was used to improve efficiency-based shifting schedule and testing different gear shifting duration times for an electric vehicle [37]. It has been studied to develop design and control algorithms on the light air bearing simulator [38]. A simulator with Vehicle in the loop was studied for a realistic driving feeling with haptic steering feedback in high speed applications [39]. A motion cueing algorithm-based model predictive controller has been studied for the hexapod with 9 DoF, which exhibits non-linear behaviour [40]. On the 2 DoF driving simulator platform capabilities and frequency response, controllability for different variations and simulator sickness were investigated [41]. A low-cost structure has been studied for a PC-based 5 DoF driving simulator, and the performance of the system under different road scenarios has been examined and it has been observed that it achieves adequate respond [42]. On the 5 DoF motorcycle riding platform, a training tool was developed for new users under different scenarios, and the behaviours and interactions of motorcycle drivers under certain conditions were studied [43]. Human mechanical impedance properties (HMIP) were investigated on 4 DoF driving simulators. Adaptive steering control is based on HMIP and its effectiveness has been tested on the double lane change scenario [44]. For a compact and low-cost driving simulator, reduction of motion clearance and correction of immersive virtual reality motion during convoy driving were evaluated [45]. An optimal tuning procedure has been tried to be developed in order to realize the expected driver behaviours during model predictive controller autonomous driving based on the motion cueing algorithm [46]. Here, mechanical configurations and system identification were studied on a new 2 DoF 3-legs driving simulator and verified with a low cost experimental setup [47]. For 5 DoF motion simulation, a new motion cueing algorithm was studied with 3 DoF motion simulators and parameter tuning was tried to be performed adaptively with an online optimization algorithm [48]. A sliding mode control based on

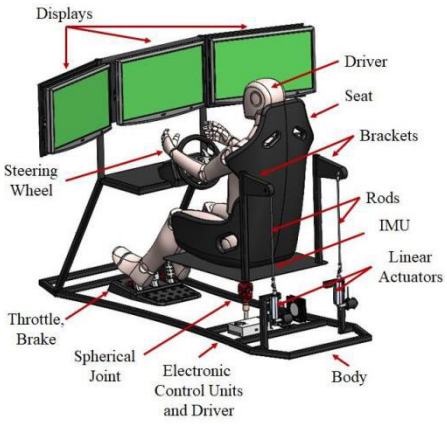

FIGURE 2. 2 DoF vehicle simulator conceptual design.

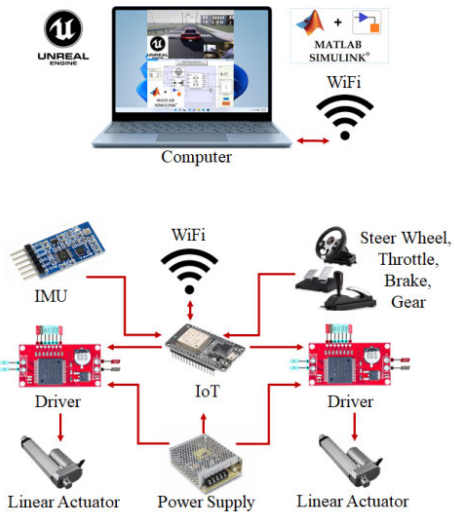

FIGURE 3. Hardware architecture of 2 DoF vehicle simulator.

FIGURE 4. 2 DoF vehicle simulator.

linear Newton-Euler dynamic equation has been developed for 3 DoF flight simulator platforms [49]. Noticeable difference corresponds to differential perception threshold is an appropriate measurement for evaluating power-train modifications. Here the motion scaling effect is analysed on the

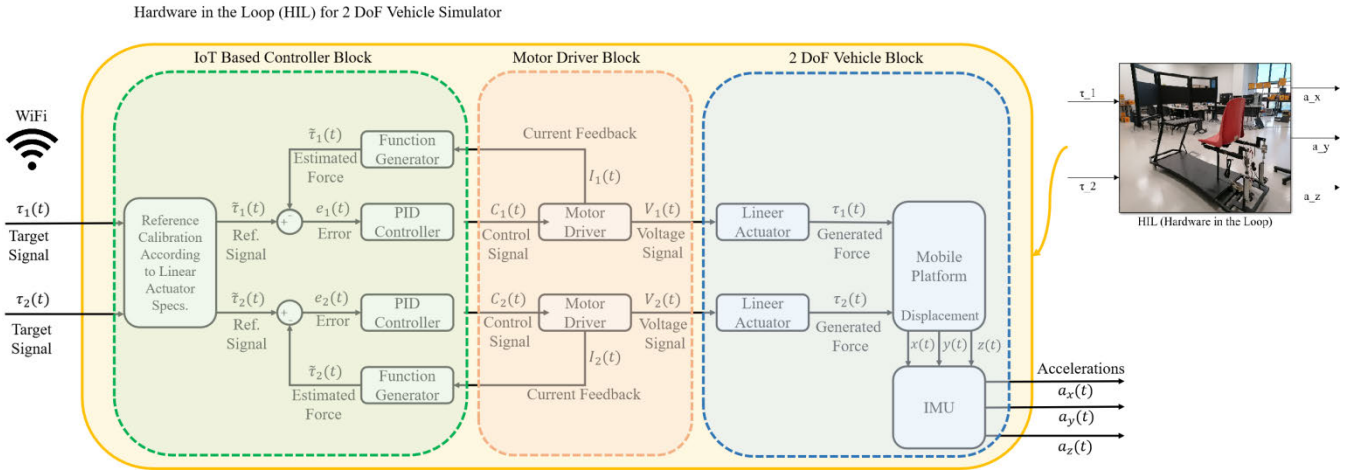

FIGURE 5. Hardware in the loop (HIL) for 2 DoF vehicle simulator.

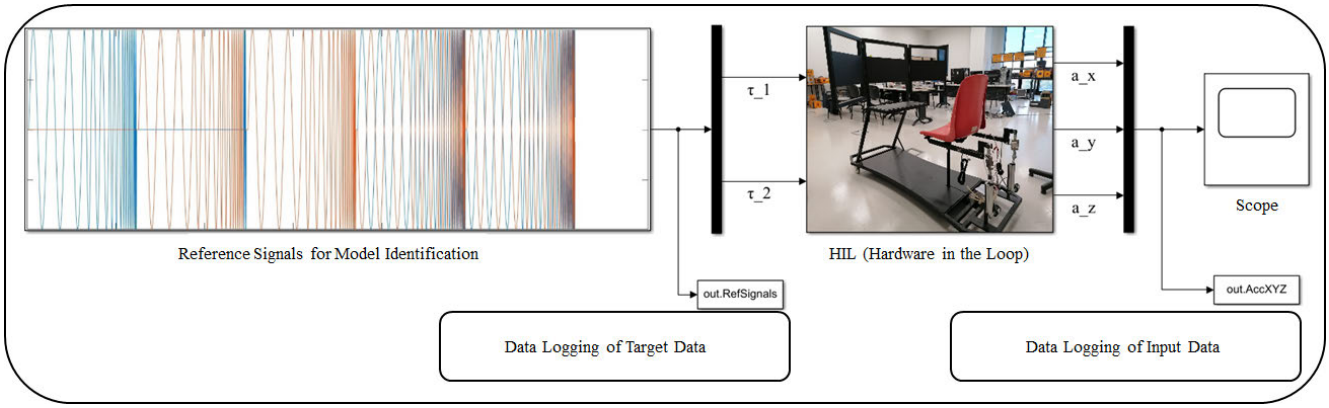

FIGURE 6. Model based system identification and training dataset generation for NN.

driving simulator. Here, it is aimed to explain the difference in perception between driving simulator and real road tests [50].

The conceptual design and hardware architecture of 2 DoF vehicle simulator as shown Fig. 2 and Fig. 3 are prototyped as shown in Fig. 4.

In this study, it was studied to determine the optimal angles of inverse kinematic-based hook joints in order to correct the mechanical errors experienced on 6 DoF vibration platforms that were previously designed [51]. Here, a spherical motion platform with multiple degrees of freedom to be controlled by sensor fusion has been studied. Since the orientation in the spherical joint is not easy to measure, the fusion of the optical sensor and IMU is used. Compensation is provided with load cells in order to prevent unstable conditions as unbalanced loads leads to the controller performance [52]. In this study, a new motion planning algorithm for motion estimation is studied on the 3 DoF foldable parallel compensation platform. A motion planning algorithm based on target motion estimation and non-uniform rational B spline has been tried to be developed [53].

As it can be understood from the literature review, many methods have been tried to deploy the real driving feeling. It has been observed that the method with the best efficient way is based on neural network. The aim of this study is the different test maneuver deployment to the vehicle simulator by using IoT and NN. This study is the first phase of a two-stage project. It was carried out to verify the deployment of 2 DoF vehicle simulators under different test scenarios. In the second phase, the deep learning algorithms for obtained test results will be studied on testing and observing in terms of the behavioural differences between healthy persons and post-operatively rehabilitated persons. In this study, the method that will contribute to the literature will be the evaluation of 3 different neural network models that will be trained with system identification data. Moreover, the improvement of the reference trajectory tracking performance will be analysed with the models to be trained with the data decomposed and composed by feature extraction by applying Fast Fourier Transform (FFT) and Inverse FFT (IFFT) of the training data. To differentiate and observe the performance of 3 different NN model besides to extract the feature of the data, FFT is

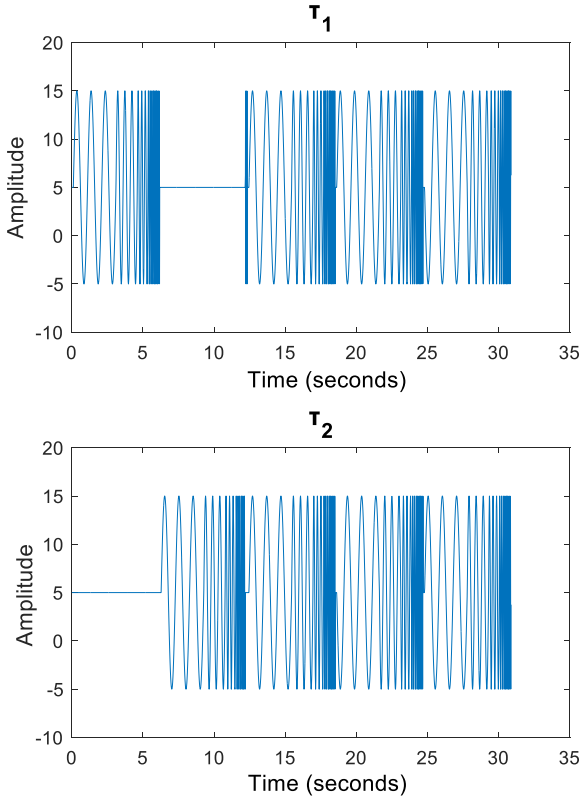

FIGURE 7. Model based system identification and training dataset generation for NN.

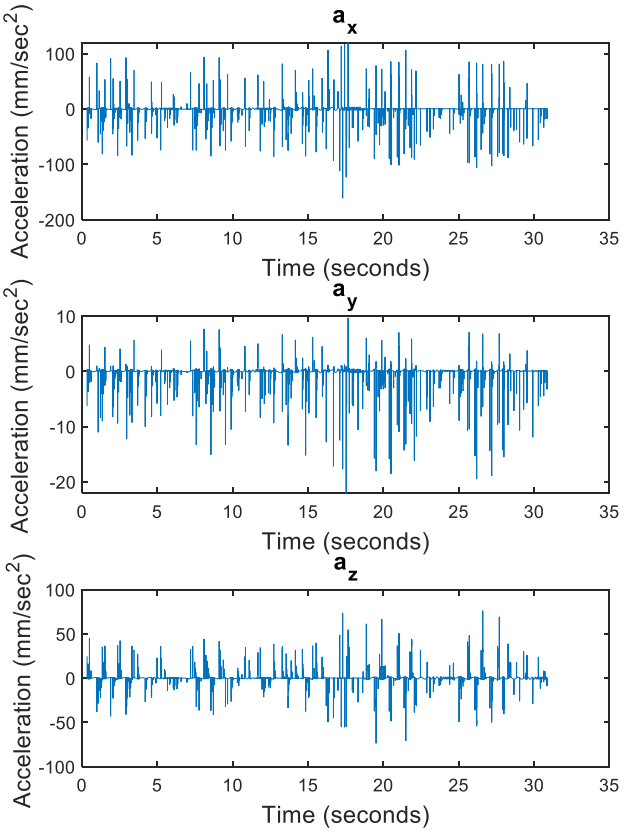

FIGURE 8. HIL responses for system identification inputs.

used for the training data set to assess the potential enhancement the realistic driving during test maneuver. And FFT provides extraction of the feature of the training data such as its amplitude and phase. Therefore, it enables more data as potential improvement. However, it has also more computing time and it may cause more latency considering the limited computing of the micro-controller hence the optimal processing has to be determined. Finally, the trained neural networks will be subjected to driving scenarios for validation and assessment.

II. 2 DoF VEHICLE SIMULATOR

The vehicle simulator has generally various degree of freedom such as 2, 3 and more. The vehicle simulators with high degrees of freedom have more complex mechanical systems and need electronic control systems that require higher computational power. In this study, 2 DoF was preferred due to the limited project budget and low cost scope. In this section, the 2 DoF vehicle simulator is presented, and the conceptual design of 2 DoF vehicle simulator is shown in Fig. 2. In 2 DoF vehicle simulator, the motion is generated using two linear actuators that are attached to the mobile platform representing the driver's seat. Acceleration data along the *x*-*y*-*z* axes is obtained as feedback through the use of an Inertial Measurement Unit (IMU). The control signals of the linear actuators and the IMU are transmitted to the host computer via an IoT. The hardware architecture of 2 DoF vehicle simulator is shown in Fig. 3.

The prototype is constructed by stainless steel. And the analysis of stress strain of the 2 DoF vehicle simulator are capable of carrying up to a driver with 80 kg.

$$\tau = M(q)\,\ddot{q} + V(q,\dot{q}) + G(q) \tag{1}$$

$$\frac{\mathrm{d}}{\mathrm{d}t}\left(\frac{\partial K}{\partial \dot{x}}\right) - \frac{\partial K}{\partial x} + \frac{\partial U}{\partial x} + \sum_{i=1}^{2} \varsigma_i G_{i1} = 0 \tag{2}$$

$$\frac{\mathrm{d}}{\mathrm{d}t}\left(\frac{\partial K}{\partial \dot{y}}\right) - \frac{\partial K}{\partial y} + \frac{\partial U}{\partial y} + \sum_{i=1}^{2} \varsigma_i G_{i2} = 0 \tag{3}$$

$$\tau_1 = \frac{d}{dt}\left(\frac{\partial K}{\partial y_1}\right) - \frac{\partial K}{\partial y_1} + \frac{\partial U}{\partial y_1} + \sum_{i=1}^{2} \varsigma_i G_{i3} \tag{4}$$

$$\tau_2 = \frac{d}{dt}\left(\frac{\partial K}{\partial y_2}\right) - \frac{\partial K}{\partial y_2} + \frac{\partial U}{\partial y_2} + \sum_{i=1}^{2} \varsigma_i G_{i4} \tag{5}$$

A mathematical model for the 2-degree-of-freedom (DoF) vehicle simulator is presented in equations (1) to (5), which integrates both kinematic and dynamic models. The model includes the positional mass matrix, M(q), the vector of nonlinear sets arising from the centripetal and Coriolis accelerations, V(q, $\dot{q}$), and the vector of gravitational terms, G(q). The total kinetic energy of the system is denoted as K, the total potential energy as U, and G_{ij} represents the Lagrange

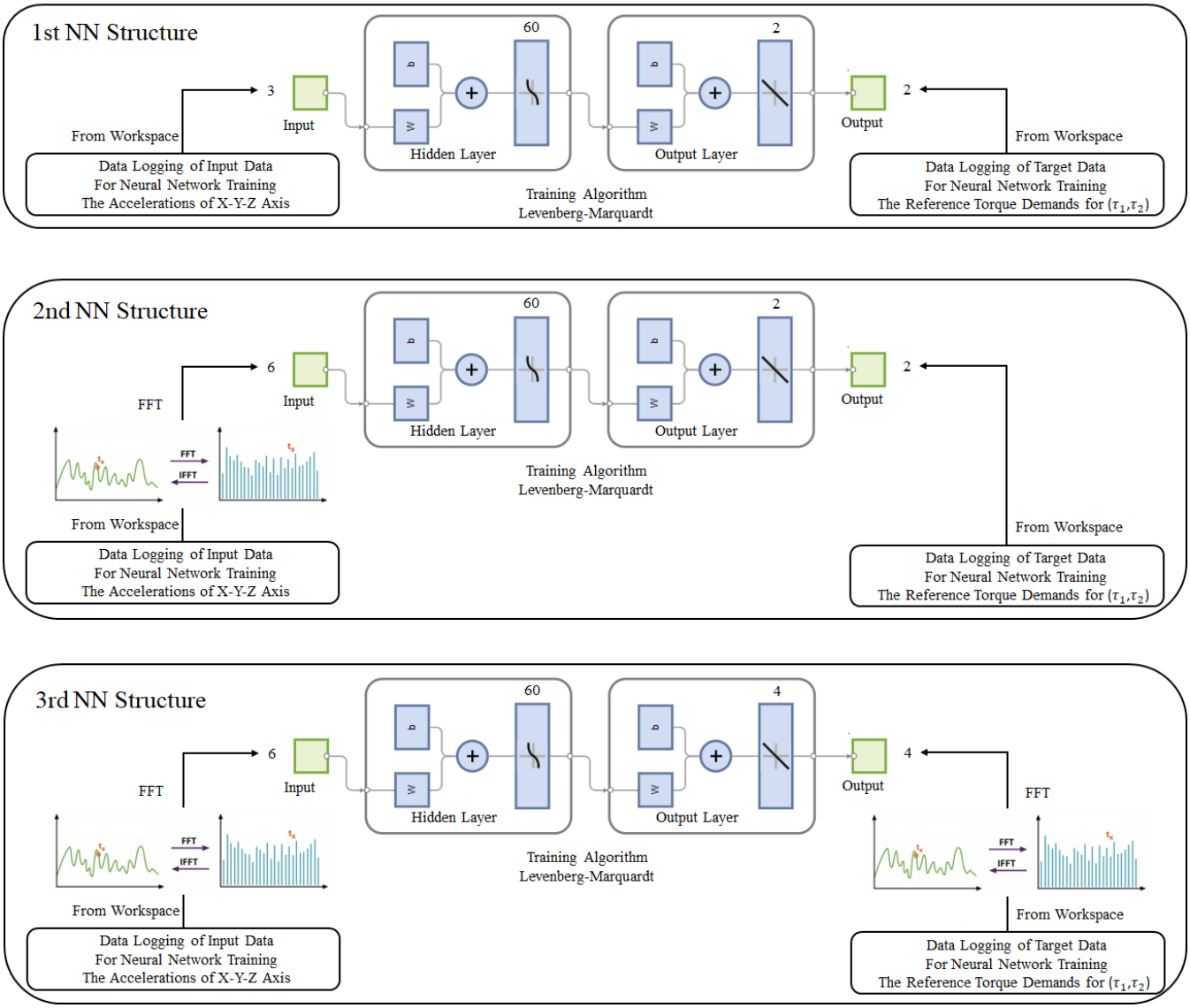

FIGURE 9. 3 Different types of NN structures.

multiplier. This model has been previously described in the literature [54], [55], [56].

In the hardware architecture shown in Figure 3, a 12V power supply, 500N force and 100mm stroke 2 linear motors with 500N force and 100mm stroke, 2 motor drivers (VNH2SP30) with 12V – 30A, ESP32-WROOM-32U as IoT, MPU9250 as IMU and Snopy V5H USB Pro as throttle-brake-steering-gear are used. The equipment cost is 4750$.

The controller block diagram as HIL with 2 inputs (Forces) and 3 Outputs (Accelerations) is shown in Fig. 5. HIL consists of 3 layer which are IoT based controller block, motor driver block, 2 DoF vehicle simulator block. Here, IoT based controller block receives the torque demand and calculates required reference of PID block. Motor driver block receive the control signal and provides feedback and motor drive signals. 2 DoF vehicle simulator is plant model and it provides the desired acceleration. The PID Controller blocks, which drives the linear actuators here, are tuned to meet the requirements of real time, considering the maximum accelerations within the scope of actuator specifications and test scenarios.

III. MATERIALS AND METHODS

In this study, the results of the data to be used for Neural Network training were used by the System identification. Here, the model-based system identification process for obtaining NN training data is shown in Fig. 6. The target data to be used for NN training are shown in Fig.7 which are defined by considering the linear actuator specifications of the linear actuator used in 2 DoF vehicle simulator and maximum acceleration values that may occur, as well as the initial positions of the linear actuators. The sinusoidal signals as shown in Fig. 7 consist of frequencies ranging from 1 to 20 Hz and 10 V

amplitudes with 5 V offset, and two-phase shift from 180 and 360 degrees are utilized. Fig. 7 shows the system identification signals, which were used to characterize the vehicle simulator system and generate the input reference signals for neural network training. Fig. 8 shows the acceleration data (a_x, a_y, a_z) obtained from the IMU on the vehicle simulator during the system identification process on the hardware-in-the-loop (HIL) setup.

The obtained accelerations (a_x, a_y, a_z) as shown in Fig. 8 change from −150mm/secII to 100mm/secII. And the maximum acceleration is observed on x-axis. On y-axis, the acceleration changes from −22mm/secII to 10mm/secII, is observed that minimum acceleration comparison with x and z axes due to the limited displacement of y-axis. On z-axis is observed that the acceleration changes from −75mm/secII to 75mm/secII.

As the growth of the NN structure increases the processing time, it directly causes the instantaneous data generation to be delayed over NN. Besides the Neural Network fitting algorithms are considered as the deployment problem of the test maneuver is based on fitting problem. The pure NN structure are preferred due to the limited computing of IoT based micro-controller and real time requirements. Therefore, 3 different neural network architectures are determined as shown in Fig. 9. Here, the training data preparation are given for all NN models. Fig. 10 shows the amplitude and phase data of the acceleration data to extract more feature for 2nd NN structure. Fig. 11 shows the amplitude and phase data of the torque data to extract more feature for 3nd NN structure. All determined NN structures consist of two layers. These are the hidden layer and the output layer. And it has been determined that 60 neurons are used in the hidden layer for the optimal results in order to avoid delays and latency due to processing time. The number of neurons in the output layer is configured according to the required output number depending on the NN structure. Here, it is considered to differentiate the input – output numbers to create 3 different NN structures. In order to achieve this, it was tried to extract the features and analyse the possibility of better learning by decomposing the data used in NN training by FFT.

All NN structures are created and trained in Matlab Toolbox then exported to Simulink environment. In the hidden layer, the number of neuron is determined by design of experiment with BBD (Box-Behnken Design) considering the minimization of the processing time of NN. The propagation time of NN is preferred lower than 1 millisecond according to the sampling time and micro-controller speed to avoid latency of the deployment process. Therefore, the maximum neuron is calculated as 80 according to the micro-controller processing cycle. According to the design constraint, structure and parameter, a BBD is performed. In BBD, the hidden layer neuron number (40,60,80), training algorithm (Bayesian Regularization, Scaled Conjugate Gradient, Levenberg-Marquardt) and NN structure (3 in-2 out, 6 in-2 out, 6 in-4 out) as the design parameters are determined for BBD. After the BBD, NN performance, MSE and

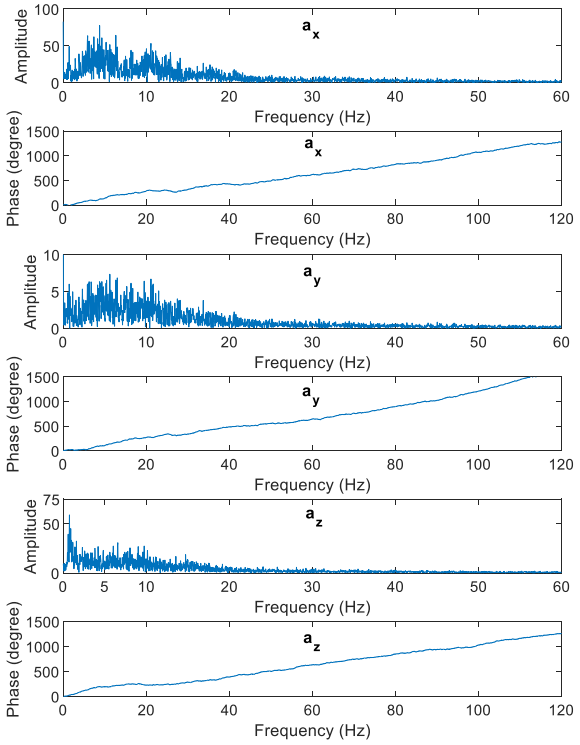

FIGURE 10. FFT results for HIL responses as training input data of NN.

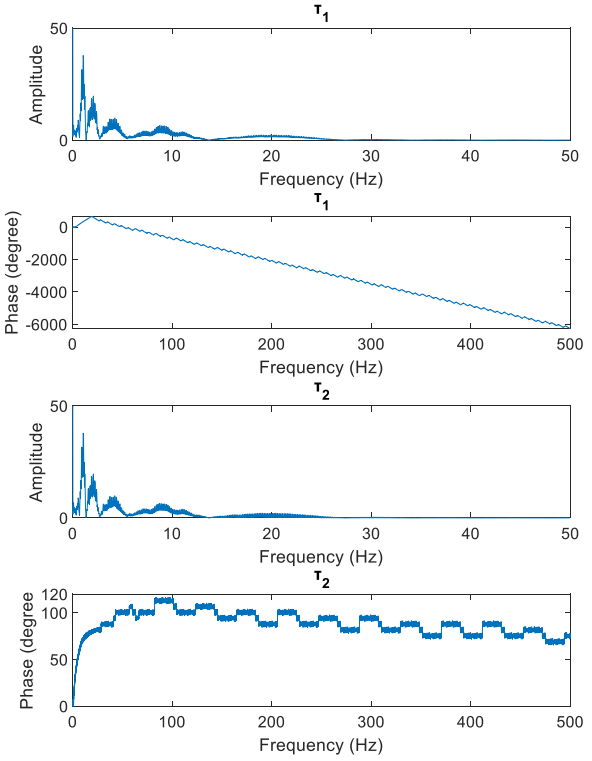

FIGURE 11. FFT results for system identification inputs as training target data of NN.

Processing Cycle are observed as results of the experiments. According to the results, 60 neurons for hidden layer and Levenberg-Marquardt for training algorithm are determined.

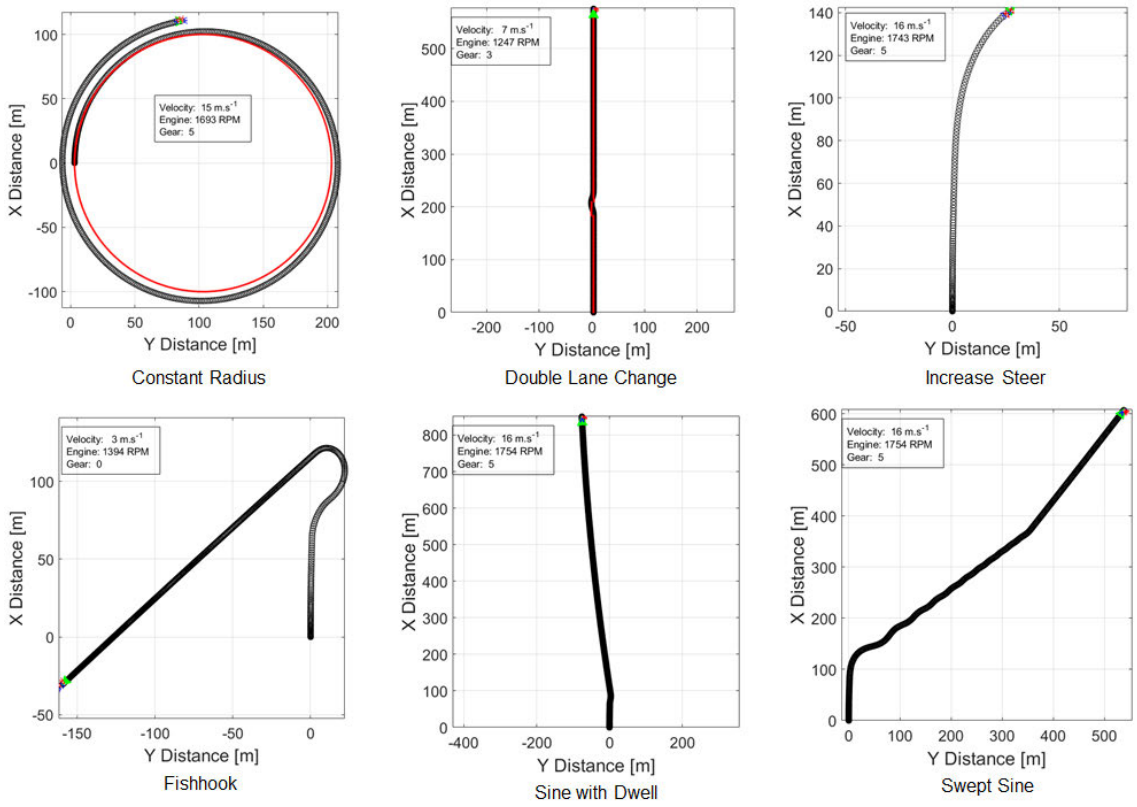

FIGURE 12. Driving scenarios.

The 1st NN structure (Fig. 9) consists of 3 inputs (a_x, a_y, a_z) and 2 outputs ($\tau 1$, $\tau 2$). It comprises two layers called hidden and output, with 60 and 2 neurons, respectively. The activation function employed in the hidden layer is Tansig, while Purelin is utilized in the output layer. The 1st NN structure is trained with the input data (Fig. 8) and target data (Fig. 7) by using the Levenberg-Marquardt algorithm.

The 2nd NN structure (Fig. 9) consists of 6 inputs (amplitudes and phases of a_x, a_y, and a_z as shown in Fig. 10) and 2 outputs ($\tau 1$, $\tau 2$), where the activation functions and training algorithm are the same as the 1st NN structure. In 2nd NN structure, 6 input data are obtained as amplitudes and phases of a_x, ay, and a_z by FFT. The 2nd NN structure is trained with the input data (Fig. 10) and target data (Fig. 7) by using the Levenberg-Marquardt algorithm.

The 3rd NN structure (Fig. 9) consists of 6 inputs (amplitudes and phases of ax, ay, and az as shown in Fig. 10) and 4 outputs (amplitudes and phases of $\tau 1$, $\tau 2$ as shown in Fig. 11). In 3rd NN structure, 6 inputs data are obtained as amplitudes and phases of a_x, a_y, and a_z by FFT, and 4 outputs data are obtained as amplitudes and phases of $\tau 1$, $\tau 2$ by FFT. It has 60 neurons in the hidden layer and 4 neurons in the output layer. Tansig and Purelin are used as activation functions in the hidden and output layers, respectively. The 3rd NN structure is trained with the input data (Fig. 10) and target data (Fig. 11) by using the Levenberg-Marquardt algorithm.

After the training of the NN structures met the desired criteria, driving scenarios are reviewed in the literature for testing and validation. Driving scenarios are often designed to measure vehicle response in different dynamic conditions. Therefore, driving scenarios consist of various maneuvering movements including acceleration, deceleration, cruise, idle mode, right and left turn. These maneuvers are typically designed to evaluate the effect of individual components or subsystems on the overall performance and handling of the vehicle. In this study, it is aimed to test the real driving feeling by transferring the vehicle responses to the driver via the 2 DoF vehicle simulator. In the literature, commonly used test procedures are determined to test and validate the trained NN structures. These test procedures are Constant Radius (CR) (SAE J266_199601 and ISO 4138:2012), Double Lane Change (DLC) (ISO 3888-2), Fishhook (FH) (NHTSA standard), Increasing Steer (IST) (SAE J266), Sine with Dwell (SwD) (NHTSA standard), and Swept Sine (SS) which are shown in Fig. 12 [57], [58], [59], [60]. The lateral and longitudinal movement of the driving scenarios as shown in Fig. 12 are used for test of all trained NN model.

To test and evaluate the NN structure performances, all driving scenarios as shown in Fig. 12 are run on reference

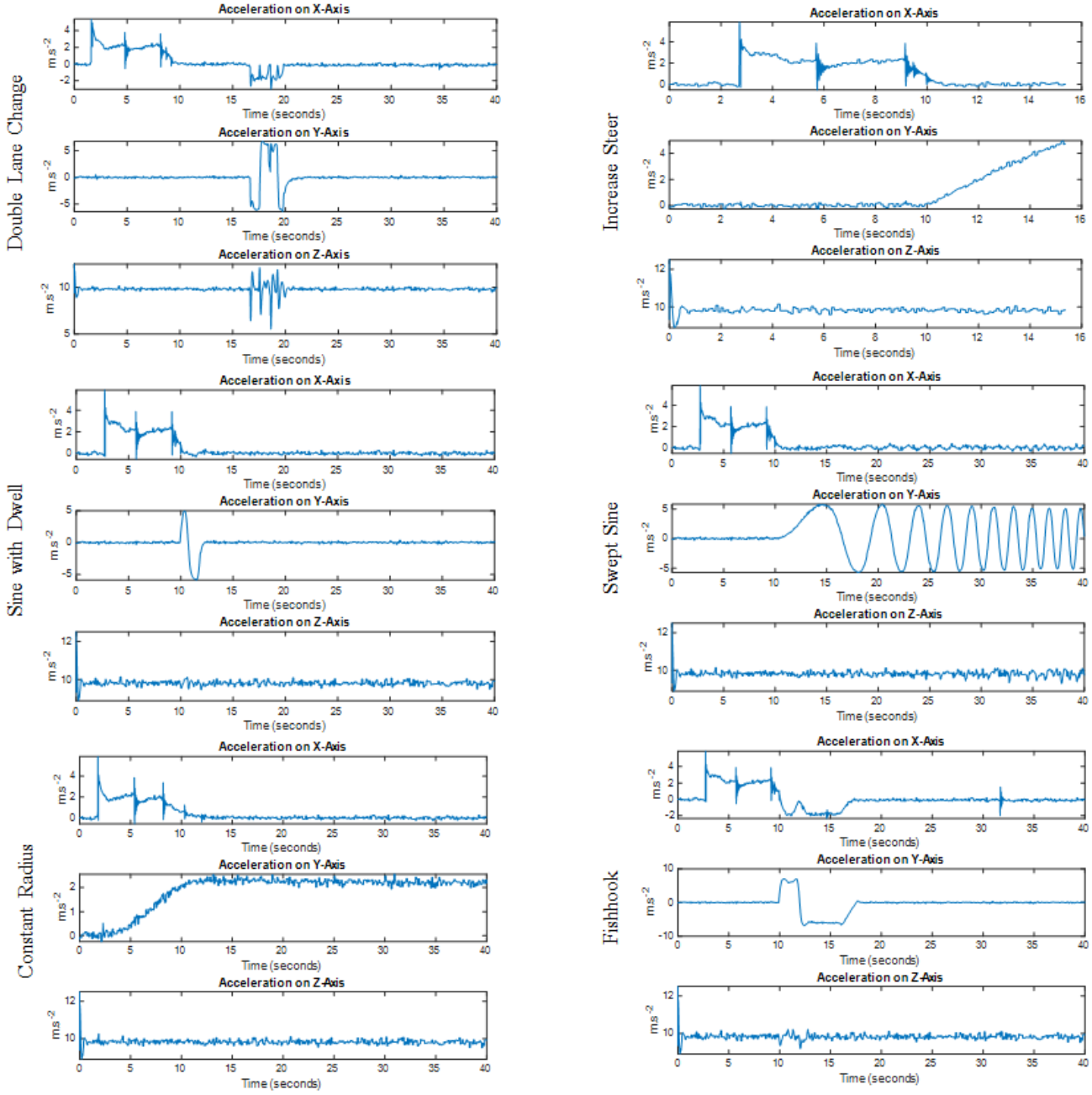

FIGURE 13. Acceleration on x-y-z axes for each driving scenarios.

application to create the test data for the NN structures. To avoid ethical permission and other undesirable situations such as sitting position, posture alignment and different weight, it is preferred maximum bulk mass (80 kg) during the tests due to the 2 DoF vehicle simulator has capable of carrying up to 80 kg.

The obtained acceleration data under the driving scenarios simulated in the reference application is presented in Fig. 13 for the x, y, and z axes. The trained neural network models are subsequently evaluated using acceleration data obtained from the test scenarios as shown in Figure 14. The test scenarios include Double Lane Change (DLC), Constant Radius (CR), Fishhook (FH), Increase Steer (IST), Sine with Dwell (SwD), and Swept Sine (SS), all of which were recorded and analysed for their respective acceleration data (a_x, a_y, a_z). After obtaining the relevant test data, the evaluation process is tested separately for each NN structure as shown in Fig. 14. Since the test data of the driving scenarios is in the time domain, the input data for the 2nd and 3rdNN structures are obtained after the FFT process and applied to the NN input.

In addition, as the output of the 3rd NN structure includes the amplitudes and phases of the control signals, these signals

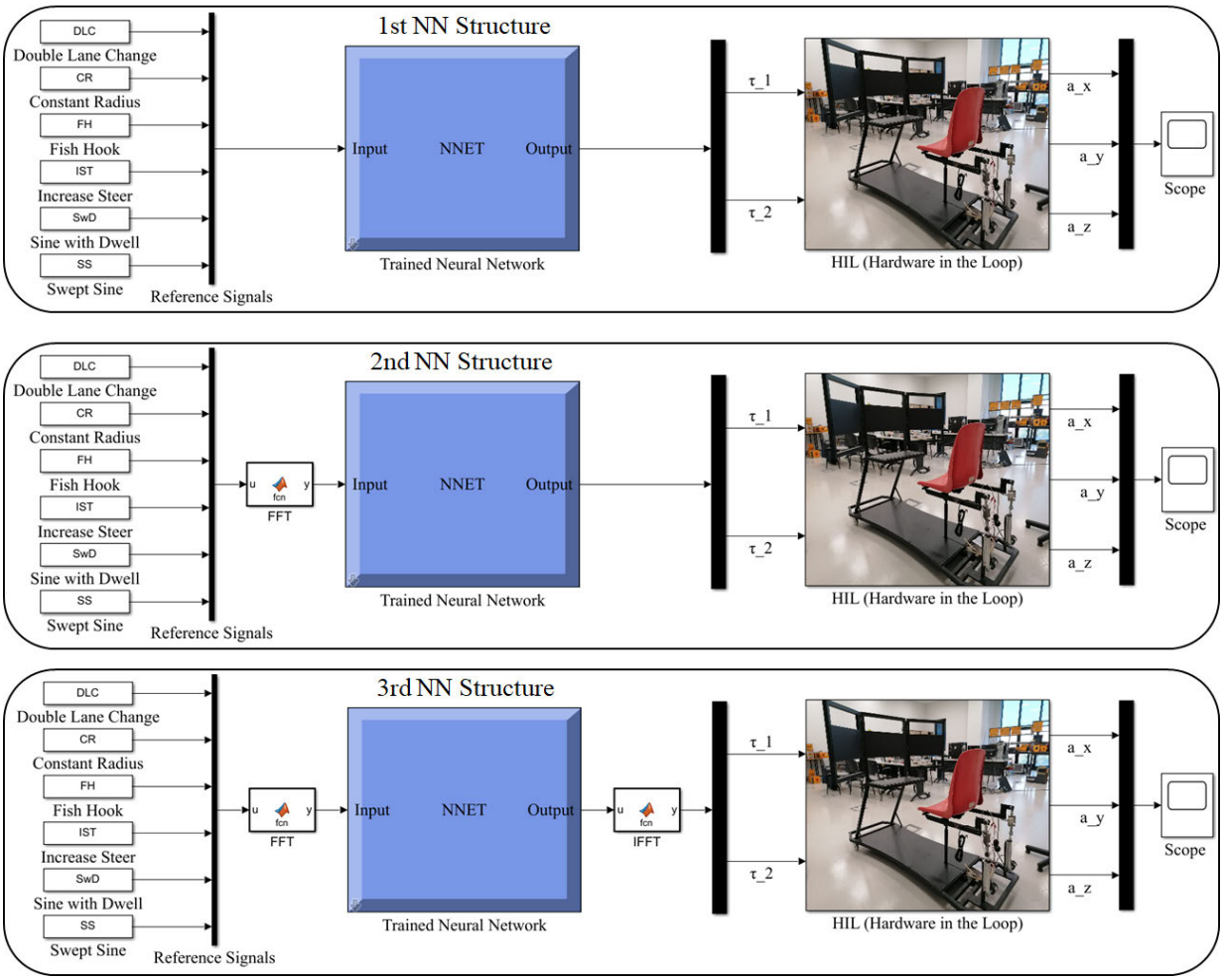

FIGURE 14. Deployment procedure to 2 DoF vehicle simulator.

are recomposed with IFFT and converted into control signals then applied to HIL.

IV. RESULTS AND DISCUSSION

The trained neural networks undergo a validation process, as illustrated in Fig. 14. In this process, the acceleration data (a_x, a_y, a_z) obtained from various test maneuvers serve as the reference signal for DLC, CR, IST, FH SwD, and SS test cases. During the testing of the reference test maneuvers on a vehicle, the acceleration data is recorded as time series. The recorded test data is then scaled according to the constraints of the vehicle simulator. The performance of the trained neural network is evaluated by separately applying the recorded acceleration data as time series to the neural network input for each test scenario. During the test phase of all NN structures, the results and reference signals obtained on each axis (x-y-z) and each NN structure (1^{st}, 2^{nd}, 3^{rd}) are shown separately in Fig. 15.

The training results of NN structures indicate a performance of 87.1% and MSE = 9.2 for the 1st NN, 91.2% and MSE = 7.8 for the 2nd NN, and 89.8% and MSE = 8.4 for the 3rd NN.

The obtained results in Fig. 15 are considered as reference and measured signals and are evaluated using the mean absolute percentage error, which is presented in Table 1. As shown in Table 1, the system verification is achieved with an average error of 13%. Since the vehicle simulator used in this study has 2 degrees of freedom, it is observed that the acceleration error on the z-axis is relatively higher compared to the acceleration errors on the *x* and *y*-axes. Moreover, the minimum and maximum errors are found to be 7% and 19%, respectively.

The results of this study indicate that the neural network structures trained using the Levenberg-Marquardt algorithm are highly effective in predicting the behaviour of vehicles under different test scenarios. The validation process produced a relatively low mean absolute percentage error, suggesting that the trained neural networks can accurately estimate the acceleration data of vehicles.

To achieve a realistic driving experience, it is imperative that the neural network is capable of computing appropriate

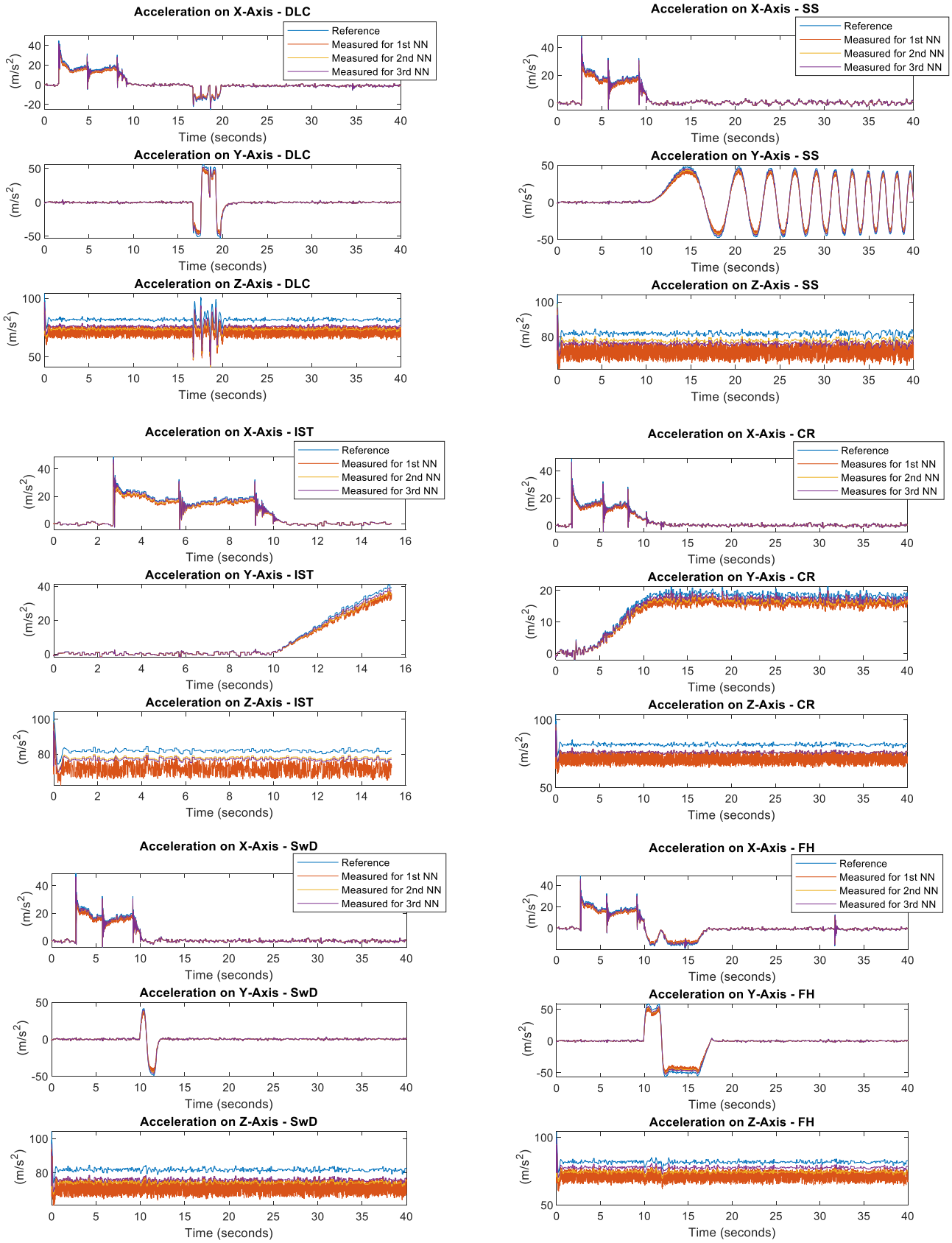

FIGURE 15. Test results of 2 DoF vehicle simulator under driving scenarios.

TABLE 1. MAPE (mean absolute percentage error) (%).

Test Scenarios	1st NN Structure			2nd NN Structure			3rd NN Structure		
	a_x	a_y	a_z	a_x	a_y	a_z	a_x	a_y	a_z
DLC	12.91%	13.00%	13.05%	9.92%	7.73%	7.33%	9.83%	9.32%	9.6%
CR	12.97%	13.00%	13.02%	7.07%	9.31%	9.42%	10.87%	9.51%	10.84%
IST	12.99%	12.97%	12.88%	9.80%	7.18%	7.43%	9.75%	10.45%	9.33%
FH	13.00%	13.11%	12.92%	8.01%	8.92%	9.92%	10.18%	10.56%	10.5%
SwD	12.96%	13.00%	13.05%	7.45%	9.27%	9.78%	10.59%	10.89%	9.82%
SS	12.95%	13.00%	13.00%	8.69%	9.93%	9.96%	10.88%	9.89%	9.73%
		Average	13.00%		Average	8.73%		Average	10.14%

control signals. However, the limited processing capacity of the micro-controller on the vehicle simulator can lead to delays and a diminished driving sensation. In order to overcome this challenge, the acquired data is transmitted to the main server via the Internet of Things (IoT) for processing in the neural network. The resulting reference signals are then transmitted back to the actuators via IoT to generate the necessary accelerations and achieve a more realistic driving experience. This approach leverages the power of cloud computing to overcome the limitations of the micro-controller and enables the neural network to compute more complex control signals with greater accuracy and precision. Such an approach has the potential to enhance the driving experience and provide more realistic testing scenarios for researchers and practitioners in the field of vehicle dynamics.

Overall, the results of this study demonstrate the potential of neural network structures for predicting the behaviour of vehicles in various test scenarios, and suggest promising avenues for further research and development in this area.

V. CONCLUSION

This study presents enhanced test maneuver deployment with feature extraction and NN for a 2 DoF vehicle simulator. The simulator must convey a realistic driving experience to the driver for different driving scenarios. This is achieved by transferring the acceleration of the axis set, which is adjusted based on the driving scenario of the relevant manipulators, to the mobile platform. To transfer the reference accelerations on the three main axes to the driver, two linear actuators on the 2 DoF vehicle simulators must be excited. To address this nonlinear problem with three inputs and two outputs, the PID controller are powered by NN-based reference signal generator is a necessary solution. Where, NN structure is used rather than inverse kinematics to derive the torque demand from accelerations.

In order to ensure a realistic driving experience, the neural network must be capable of computing suitable control signals. However, the micro-controller on the vehicle simulator has limited processing capacity, which can result in delays and a reduced driving sensation. To overcome this, the acquired data is transmitted to the main server via IoT for processing in the neural network. The resulting reference signals are then sent back to the actuators via IoT to generate the appropriate accelerations and achieve a realistic driving experience.

Once the IoT and neural network-based simulator has been set up and the neural network trained using data acquisition and system identification techniques, the system's performance is verified through various driving maneuvers such as DLC, CR, IST, FH, SwD, and SS.

To train the neural network, the vehicle simulator is exposed to two different combination signals with frequencies ranging from 1 to 20 Hz, as well as two different combinations of phase shifts (180 and 360 degrees). The resulting accelerations on the driver's seat are recorded, with the applied control signals serving as target data for the neural network, and the acceleration data serving as input data.

To evaluate the convergence of different neural network structures to the reference input, three different types of structures are used in this study. The 1st NN structure has three inputs (the accelerations) and two outputs (the force demands). The 2nd NN structure has six inputs (the phase angle and amplitude of the accelerations obtained via FFT) and two outputs (the force demands). The 3rd NN structure also has six inputs (the phase angle and amplitude of the accelerations) and four outputs (the phase angle and amplitude of the force demands obtained via FFT). In the 3rd NN structure, the outputs are re-composed by IFFT to obtain the force demands for the actuators.

The neural network structures used in this study consist of 3-6-6 inputs (1st NN - 2nd NN - 3rd NN), 2-2-4 outputs (1st NN - 2nd NN - 3rd NN), and 2 layers. Tansig activation function with 60 neurons in the hidden layer is preferred for the neural network, while purelin activation functions are preferred with 2-2-4 neurons (1st NN - 2nd NN - 3rd NN) in the output layer. The neural network is trained using the Levenberg-Marquardt training algorithm with the logged data. The performances of the 1st, 2nd, and 3rd NN structures are evaluated, and the results show that the 2nd NN structure has the best performance, achieving 91.2% accuracy and an

MSE of 7.8, while the 1st and 3rd NN structures achieve 87.1% accuracy with an MSE of 9.2 and 89.8% accuracy with an MSE of 8.4, respectively.

During the test phase, the recorded acceleration data from real vehicle driving maneuvers such as DLC, CR, IST, FH, SwD, and SS are scaled and processed, then applied to the neural network as input. The output control signals generated by the neural network are transferred to the actuators of the vehicle simulators via IoT. The performance of the system is evaluated by transferring the measured acceleration data from the IMU on the driver's seat to the main server via IoT. The results show that the vehicle simulator can track the reference accelerations with an average error of 13%, 8.73%, and 10.14%, which is acceptable for this type of system. The maximum error observed during the assessments is 19%.

The 2nd NN structure outperforms the 1st and 3rd NN structures due to its ability to better train for reference inputs such as amplitude and phase angle. On the other hand, the 3rd NN structure shows better convergence compared to the 1st NN structure. A summary of the MAPE results for the applied reference accelerations and the measured accelerations is presented in Table 1.

The finding is significant for researchers and practitioners in the field of vehicle dynamics, as it provides a promising approach for predicting a vehicle's behaviour under various test scenarios.

Moreover, this study provides a foundation for further exploration of the performance of trained neural networks on different vehicle simulators. Future studies could investigate the robustness of the proposed approach and evaluate its potential for predicting vehicle behaviour under various conditions. Additionally, incorporating additional features, such as road conditions or the vehicle's speed, could further enhance the accuracy of the trained neural networks.

REFERENCES

[1] S. Kharrazi, B. Augusto, and N. Fröjd, "Vehicle dynamics testing in motion based driving simulators," *Vehicle Syst. Dyn.*, vol. 58, no. 1, pp. 92–107, Jan. 2020, doi: 10.1080/00423114.2019.1566555.

[2] S. T. C. I. Wimaladharma, A. G. A. Sampath, J. D. B. Sampath, and C. H. V. Sapumohotti, "A game-based driving learning system for sri Lankan driving learners to enrich the awareness of road rules," in *Proc. Int. Conf. High Perform. Big Data Intell. Syst. (HPBDIS)*, May 2019, pp. 195–199, doi: 10.1109/HPBDIS.2019.8735443.

[3] L. Wang, J. Jiang, and M. Wang, "Research on MPC control of a 6 DOF Stewart platform," in *Proc. IEEE Int. Conf. Manipulation, Manuf. Meas. Nanosc. (3M-NANO)*, Tianjin, China, Aug. 2022, pp. 65–69, doi: 10.1109/3M-NANO56083.2022.9941574.

[4] Y. Zhou, J. She, F. Wang, and M. Iwasaki, "Disturbance rejection for Stewart platform based on integration of equivalent-input-disturbance and sliding-mode control methods," *IEEE/ASME Trans. Mechatronics*, early access, Feb. 6, 2023, doi: 10.1109/TMECH.2023.3237135.

[5] S. Kulothungan, R. V. Anirudh, K. Sivashankar, and A. K. Dash, "Design and development of a vehicle dynamics model for a drive simulator," in *Proc. 3rd Int. Conf. Commun. Electron. Syst. (ICCES)*, Coimbatore, India, Oct. 2018, pp. 153–156, doi: 10.1109/CESYS.2018.8723987.

[6] M. K. Safeena, K. S. Jiji, and P. R. Kumar, "Adaptive super twisting control of Stewart platform based on super twisting observer," in *Proc. IEEE 19th India Council Int. Conf. (INDICON)*, Kochi, India, Nov. 2022, pp. 1–6, doi: 10.1109/INDICON56171.2022.10040135.

[7] S. Yi, Z. Jiang, H. Chen, X. Ma, and Q. Zhang, "Hybrid micropositioning and microvibration isolation control of a multi-DOF Stewart platform," in *Proc. 34th Chin. Control Decis. Conf. (CCDC)*, Hefei, China, Aug. 2022, pp. 1314–1319, doi: 10.1109/CCDC55256.2022.10034262.

[8] A. Elkenawy, A. M. El-Nagar, M. El-Bardini, and N. M. El-Rabaie, "Full-state neural network observer-based hybrid quantum diagonal recurrent neural network adaptive tracking control," *Neural Comput. Appl.*, vol. 33, no. 15, pp. 9221–9240, Aug. 2021, doi: 10.1007/s00521-020-05685-x.

[9] A. Ozcan, C. Catal, E. Donmez, and B. Senturk, "A hybrid DNN–LSTM model for detecting phishing URLs," *Neural Comput. Appl.*, vol. 35, no. 7, pp. 4957–4973, Mar. 2023, doi: 10.1007/s00521-021-06401-z.

[10] X. Jiang, J. Wang, Q. Meng, M. Saada, and H. Cai, "An adaptive multi-class imbalanced classification framework based on ensemble methods and deep network," *Neural Comput. Appl.*, pp. 1–19, Feb. 2023, doi: 10.1007/s00521-023-08290-w.

[11] A. Nighojkar, A. Plappally, and W. Soboyejo, "Neural network models for simulating adsorptive eviction of metal contaminants from effluent streams using natural materials (NMs)," *Neural Comput. Appl.*, vol. 35, no. 8, pp. 5751–5767, Mar. 2023, doi: 10.1007/s00521-023-08315-4.

[12] D. L. de Vargas, J. T. Oliva, M. Teixeira, D. Casanova, and J. L. G. Rosa, "Feature extraction and selection from electroencephalogram signals for epileptic seizure diagnosis," *Neural Comput. Appl.*, pp. 1–25, Feb. 2023, doi: 10.1007/s00521-023-08350-1.

[13] S. D. C. A. Basílio, C. M. Saporetti, and L. Goliatt, "An interdependent evolutionary machine learning model applied to global horizontal irradiance modeling," *Neural Comput. Appl.*, pp. 1–22, Feb. 2023, doi: 10.1007/s00521-023-08342-1.

[14] A. K. Gupta and R. Johari, "IoT based electrical device surveillance and control system," in *Proc. 4th Int. Conf. Internet Things, Smart Innov. Usages (IoT-SIU)*, Apr. 2019, pp. 1–5, doi: 10.1109/IoT-SIU.2019.8777342.

[15] A. Sakalli, O. Aktekin, and U. Kiran, "Hardware in the loop (HiL) testing of a human electric hybrid vehicle," in *Proc. IEEE Int. Conf. Ind. Technol. (ICIT)*, Lyon, France, Feb. 2018, pp. 193–198, doi: 10.1109/ICIT.2018.8352175.

[16] M. R. Ashouri, A. Nahvi, and S. Azadi, "Time delay analysis of vehicle handling variables for near-crash detection of drowsy driving using a bus driving simulator," in *Proc. 6th RSI Int. Conf. Robot. Mechatronics (IcRoM)*, Tehran, Iran, Oct. 2018, pp. 243–249, doi: 10.1109/ICRoM.2018.8657519.

[17] M. R. C. Qazani, H. Asadi, S. Pedrammehr, and S. Nahavandi, "Performance analysis and dexterity monitoring of hexapod-based simulator," in *Proc. 4th Int. Conf. Control, Autom. Robot. (ICCAR)*, Auckland, New Zealand, Apr. 2018, pp. 226–231, doi: 10.1109/ICCAR.2018.8384675.

[18] T. Gyorgy and D. Fodorean, "Human-in-the-loop simulation of an electric vehicle drivetrain," in *Proc. XIII Int. Conf. Electr. Mach. (ICEM)*, Alexandroupoli, Greece, Sep. 2018, pp. 1545–1550, doi: 10.1109/ICELMACH.2018.8506855.

[19] G. Markkula, R. Romano, A. H. Jamson, L. Pariota, A. Bean, and E. R. Boer, "Using driver control models to understand and evaluate behavioral validity of driving simulators," *IEEE Trans. Human-Mach. Syst.*, vol. 48, no. 6, pp. 592–603, Dec. 2018, doi: 10.1109/THMS.2018.2848998.

[20] A. I. Aulia, N. P. A. K. Rata, M. Amin, H. Hindersah, and E. Hidayat, "Throttle, motion Cueing, and platform control systems of 3-DOF locomotive simulator," in *Proc. IEEE 8th Int. Conf. Syst. Eng. Technol. (ICSET)*, Bandung, Indonesia, Oct. 2018, pp. 67–72, doi: 10.1109/ICSEngT.2018.8606379.

[21] C. Zhao, S. Li, F. Liu, W. Wang, and J. Gong, "Influence analysis of autonomous cars' cut-in behavior on human drivers in a driving simulator," in *Proc. IEEE Intell. Vehicles Symp. (IV)*, Changshu, China, Jun. 2018, pp. 85–90, doi: 10.1109/IVS.2018.8500705.

[22] Z. Szalay, M. Szalai, B. Toth, T. Tettamanti, and V. Tihanyi, "Proof of concept for scenario-in-the-loop (SciL) testing for autonomous vehicle technology," in *Proc. IEEE Int. Conf. Connected Vehicles Expo (ICCVE)*, Graz, Austria, Nov. 2019, pp. 1–5, doi: 10.1109/ICCVE45908.2019.8965086.

[23] T. Miunske, C. Holzapfel, E. Baumgartner, and H.-C. Reuss, "A new approach for an adaptive linear quadratic regulated motion Cueing algorithm for an 8 DoF full motion driving simulator," in *Proc. Int. Conf. Robot. Autom. (ICRA)*, Montreal, QC, Canada, May 2019, pp. 497–503, doi: 10.1109/ICRA.2019.8794109.

[24] L. Bruck, S. Veldhuis, and A. Emadi, "Selection method of a driving simulator motion system," in *Proc. IEEE Transp. Electrific. Conf. Expo (ITEC)*, Detroit, MI, USA, Jun. 2019, pp. 1–6, doi: 10.1109/ITEC.2019.8790465.

[25] A. I. Aulia, M. F. Fahmi, H. Hindersah, A. S. Rohman, and E. M. I. Hidayat, "Implementation of motion Cueing and motor position control for vehicle simulator with 4-DOF-platform," in *Proc. 6th Int. Conf. Electr. Veh. Technol. (ICEVT)*, Bali, Indonesia, Nov. 2019, pp. 40–45, doi: 10.1109/ICEVT48285.2019.8994028.

[26] Z. Medenica, R. Miucic, and M. Andrews, "Integrating a real vehicle into a physics-based driving simulator for human-machine interaction research," in *Proc. 12th Int. Conf. Hum. Syst. Interact. (HSI)*, Richmond, VA, USA, Jun. 2019, pp. 174–178, doi: 10.1109/HSI47298.2019.8942616.

[27] J. Cheng, H. Su, and K. Chen, "Driver posture detection method in motorcycle simulator," in *Proc. Int. Conf. Artif. Intell. Adv. Manuf. (AIAM)*, Dublin, Ireland, Oct. 2019, pp. 622–626, doi: 10.1109/AIAM48774.2019.00129.

[28] H. Asadi, A. Mohammadi, S. Mohamed, M. R. C. Qazani, C. P. Lim, A. Khosravi, and S. Nahavandi, "A model predictive control-based motion Cueing algorithm using an optimized nonlinear scaling for driving simulators," in *Proc. IEEE Int. Conf. Syst., Man Cybern. (SMC)*, Bari, Italy, Oct. 2019, pp. 1245–1250, doi: 10.1109/SMC.2019.8914597.

[29] A. Adel, M. Mahmoud, N. Sayed, O. Hisham, O. Ossama, P. Adel, Y. Ayman, M. I. Awad, S. A. Maged, S. M. Umer, H. Iqbal, and H. F. Maqbool, "Design of a 6-DOF hydraulic vehicle driving simulator," in *Proc. Int. Conf. Innov. Trends Commun. Comput. Eng. (ITCE)*, Aswan, Egypt, Feb. 2020, pp. 170–175, doi: 10.1109/ITCE48509.2020.9047787.

[30] H. Kanchwala and J. S. Dhillon, "A real-time hardware-in-the-loop vehicle simulator," in *Proc. IEEE 18th Int. Conf. Ind. Informat. (INDIN)*, Warwick, U.K., Jul. 2020, pp. 182–187, doi: 10.1109/INDIN45582.2020.9442138.

[31] D. Kim and S.-H. Hwang, "Kinematic implementation of 3-DOF 2-link type vehicle simulator: Kinematic analysis and motion control method for 3-DOF 2-link type vehicle simulator," in *Proc. Int. Conf. Control, Autom. Diagnosis (ICCAD)*, Paris, France, Oct. 2020, pp. 1–6, doi: 10.1109/ICCAD49821.2020.9260532.

[32] A. B. Koyuncu, E. Ercelik, E. Comulada-Simpson, J. Venrooij, M. Kaboli, and A. Knoll, "A novel approach to neural network-based motion Cueing algorithm for a driving simulator," in *Proc. IEEE Intell. Vehicles Symp. (IV)*, Las Vegas, NV, USA, Oct. 2020, pp. 2118–2125, doi: 10.1109/IV47402.2020.9304825.

[33] P. Makarun, G. Josipović, M. Švec, and Š. Ileš, "Testing predictive vehicle dynamics control algorithms using a scaled remote controlled car and a roadway simulator," in *Proc. Int. Conf. Electr. Drives Power Electron. (EDPE)*, Dubrovnik, Croatia, Sep. 2021, pp. 177–182, doi: 10.1109/EDPE53134.2021.9604086.

[34] D. Jung, "A minimally configured hardware-in-the-loop simulator of electrical power steering system for human driver interaction on crosswind effect," *IEEE Access*, vol. 9, pp. 60470–60481, 2021, doi: 10.1109/ACCESS.2021.3073989.

[35] Y. Kusakari, S. Oikawa, Y. Matsui, and N. Kubota, "Effect of human–machine interface of a vehicle on right-turn maneuver at intersections using a driving simulator," in *Proc. IEEE Int. Conf. Syst., Man, Cybern. (SMC)*, Melbourne, VIC, Australia, Oct. 2021, pp. 1607–1612, doi: 10.1109/SMC52423.2021.9659015.

[36] I. Šolc, P. Makarun, J. K. Hromatko, and Š. Ileš, "Testing direct yaw moment control using a scaled car and a roadway simulator," in *Proc. 45th Jubilee Int. Conv. Inf., Commun. Electron. Technol. (MIPRO)*, Opatija, Croatia, May 2022, pp. 800–805, doi: 10.23919/MIPRO55190.2022.9803431.

[37] E. Louback, F. Machado, L. Bruck, P. J. Kollmeyer, and A. Emadi, "Real-time performance and driveability analysis of a clutchless multi-speed gearbox for battery electric vehicle applications," in *Proc. IEEE Transp. Electrific. Conf. Expo (ITEC)*, Anaheim, CA, USA, Jun. 2022, pp. 1041–1046, doi: 10.1109/ITEC53557.2022.9814032.

[38] S. Deng, J. Zhi, H. Cai, Z. Chen, and Y. Wang, "The design and analysis of light passive air-bearing simulator," in *Proc. 6th Int. Conf. Robot. Autom. Sci. (ICRAS)*, Wuhan, China, Jun. 2022, pp. 152–156, doi: 10.1109/ICRAS55217.2022.9841971.

[39] E. Weiss and J. C. Gerdes, "High speed emulation in a vehicle-in-the-loop driving simulator," *IEEE Trans. Intell. Vehicles*, vol. 8, no. 2, pp. 1826–1836, Feb. 2023, doi: 10.1109/TIV.2022.3162549.

[40] M. Bruschetta, F. Maran, and A. Beghi, "A nonlinear, MPC-based motion Cueing algorithm for a high-performance, nine-DOF dynamic simulator platform," *IEEE Trans. Control Syst. Technol.*, vol. 25, no. 2, pp. 686–694, Mar. 2017, doi: 10.1109/TCST.2016.2560120.

[41] H. Arioui, S. Hima, L. Nehaoua, R. J. V. Bertin, and S. Espié, "From design to experiments of a 2-DOF vehicle driving simulator," *IEEE Trans. Veh. Technol.*, vol. 60, no. 2, pp. 357–368, Feb. 2011, doi: 10.1109/TVT.2010.2090675.

[42] A. R. W. Huang and C. Chen, "A low-cost driving simulator for full vehicle dynamics simulation," *IEEE Trans. Veh. Technol.*, vol. 52, no. 1, pp. 162–172, Jan. 2003, doi: 10.1109/TVT.2002.807157.

[43] H. Arioui, L. Nehaoua, S. Hima, N. Séguy, and S. Espié, "Mechatronics, design, and modeling of a motorcycle riding simulator," *IEEE/ASME Trans. Mechatronics*, vol. 15, no. 5, pp. 805–818, Oct. 2010, doi: 10.1109/TMECH.2009.2035499.

[44] Y. Tanaka, N. Yamada, T. Tsuji, and T. Suetomi, "Vehicle active steering control system based on human mechanical impedance properties of the arms," *IEEE Trans. Intell. Transp. Syst.*, vol. 15, no. 4, pp. 1758–1769, Aug. 2014, doi: 10.1109/TITS.2014.2312458.

[45] L. Nehaoua, H. Mohellebi, A. Amouri, H. Arioui, S. Espié, and A. Kheddar, "Design and control of a small-clearance driving simulator," *IEEE Trans. Veh. Technol.*, vol. 57, no. 2, pp. 736–746, Mar. 2008, doi: 10.1109/TVT.2007.905336.

[46] M. Bruschetta, C. Cenedese, A. Beghi, and F. Maran, "A motion Cueing algorithm with look-ahead and driver characterization: Application to vertical car dynamics," *IEEE Trans. Human-Mach. Syst.*, vol. 48, no. 1, pp. 6–16, Feb. 2018, doi: 10.1109/THMS.2017.2776207.

[47] C. Zhang and L. Zhang, "Kinematics analysis and workspace investigation of a novel 2-DOF parallel manipulator applied in vehicle driving simulator," *Robot. Comput.-Integr. Manuf.*, vol. 29, no. 4, pp. 113–120, Aug. 2013, doi: 10.1016/j.rcim.2012.11.005.

[48] Y.-H. Chang, C.-S. Liao, and W.-H. Chieng, "Optimal motion Cueing for 5-DOF motion simulations via a 3-DOF motion simulator," *Control Eng. Pract.*, vol. 17, no. 1, pp. 170–184, Jan. 2009, doi: 10.1016/j.conengprac.2008.05.016.

[49] D. Wu and H. Gu, "Adaptive sliding control of six-DOF flight simulator motion platform," *Chin. J. Aeronaut.*, vol. 20, no. 5, pp. 425–433, 2007, doi: 10.1016/S1000-9361(07)60064-8.

[50] E. Baumgartner, A. Ronellenfitsch, H.-C. Reuss, and D. Schramm, "A perceptual approach for evaluating vehicle drivability in a dynamic driving simulator," *Transp. Res. F, Traffic Psychol. Behav.*, vol. 63, pp. 83–92, May 2019, doi: 10.1016/j.trf.2019.03.013.

[51] I. Hostens, J. Anthonis, and H. Ramon, "New design for a 6 DoF vibration simulator with improved reliability and performance," *Mech. Syst. Signal Process.*, vol. 19, no. 1, pp. 105–122, Jan. 2005, doi: 10.1016/j.ymssp.2003.10.001.

[52] S.-M. Lee and H. Son, "Multi-sensor integration and fusion for control of multi-DOF spherical motion platform," *Mechatronics*, vol. 77, Aug. 2021, Art. no. 102593, doi: 10.1016/j.mechatronics.2021.102593.

[53] C. Wang, T. Zhao, J. Zhang, E. Li, Y. Zhao, and K. Li, "A novel motion planning algorithm for a three DoF foldable parallel compensation platform based on prediction and B-spline," *Ocean Eng.*, vol. 266, Dec. 2022, Art. no. 112876, doi: 10.1016/j.oceaneng.2022.112876.

[54] M. H. Hadian, M. Salehian, I. Sharifi, and M. B. Menhaj, "Utilizing function approximation technique and neural network controllers on a 2-DOF painter robot," in *Proc. 10th RSI Int. Conf. Robot. Mechatronics (ICRoM)*, Tehran, Iran, Nov. 2022, pp. 202–208, doi: 10.1109/ICRoM57054.2022.10025162.

[55] H. Wu, Y. Wei, X. Lian, X. Luo, C. Peng, and B. Li, "Development of an experimental platform for 3-DOF planar parallel robots," in *Proc. 5th World Conf. Mech. Eng. Intell. Manuf. (WCMEIM)*, Ma'anshan, China, Nov. 2022, pp. 840–843, doi: 10.1109/WCMEIM56910.2022.10021546.

[56] S. S. Ganesh and A. B. K. Rao, "Kinematic and dynamic optimization of a 2-DOF parallel kinematic mechanism," *Proc. Comput. Sci.*, vol. 133, pp. 576–584, Jan. 2018, doi: 10.1016/j.procs.2018.07.086.

[57] S. S. Shadrin and D. A. Makarova, "The concept of highly automated vehicles safety monitoring in operation using virtual testing procedures," in *Proc. Syst. Signals Generating Process. Field Board Commun.*, Moscow, Russia, Mar. 2022, pp. 1–6, doi: 10.1109/IEEECONF53456.2022.9744309.

[58] *J266: Steady-State Directional Control Test Procedures for Passenger Cars and Light Trucks*, SAE Int., Warrendale, PA, USA, 2018.

[59] C. Zappacosta, L. Bocciolini, F. Piccioli, M. Macherelli, D. Massini, and N. Vanni, "Overview of measurement chain and instrumentation setup for running dynamics on-track tests—Normal method—According to EN-14363 standard," in *Proc. AEIT Int. Annu. Conf. (AEIT)*, Florence, Italy, Sep. 2019, pp. 1–6, doi: 10.23919/AEIT.2019.8893424.

[60] L. Prochowski, M. Ziubinski, and M. Gidlewski, "Experimental and analytic determining of changes in motor cars' positions in relation to each other during a crash test carried out to the FMVSS 214 procedure," in *Proc. XI Int. Sci.-Tech. Conf. Automot. Saf.*, Žastá, Slovakia, Apr. 2018, pp. 1–5, doi: 10.1109/AUTOSAFE.2018.8373302.

UĞUR DEMİR received the Ph.D. degree in mechatronics engineering from Marmara University, in 2018. He is currently an Associate Professor with the Department of Mechatronics Engineering, Marmara University. He has worked extensively on the development of novel electrical machine technologies for electric vehicle traction operations and mechatronics systems. His research interests include electromagnetic actuator designs, the design optimization of electrical machines, artificial neural network applications, autonomous driving, and advanced driving technologies.

GAZİ AKGÜN was born in Denizli, Turkey, in 1982. He received the B.Sc. degree in electrical education from Dicle University, Batman, Turkey, in 2004, and the M.Sc. and Ph.D. degrees in mechatronics engineering from Marmara University, Istanbul, in 2015 and 2019, respectively. From 2005 to 2021, he was a Vocational Technical Teacher in various cities around Turkey for the National Educational Ministry. Currently, he is an Assistant Professor with the Department of Mechatronics Engineering, Marmara University. His research interests include adaptive control, predictive control, and AI supported intelligent control systems, particularly in the fields of biomechatronics and rehabilitation robotics.

MUSTAFA CANER AKÜNER received the Ph.D. degree in electrical education from Marmara University, in 1999. He is currently a Full Professor with the Department of Mechatronics Engineering, Marmara University. His research interests include electrical machines, battery electric vehicle, hybrid electric vehicle, and sustainable energy technologies.

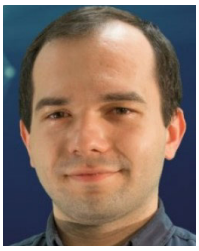

BORA DEMİRCİ received the B.S. degree in mechatronics, robotics and automation engineering from Kocaeli University, Turkey, in 2017, and the M.Sc. degree in mechatronics engineering from Marmara University, Istanbul, Turkey, in 2022, where he is currently pursuing the Ph.D. degree with the Mechatronics Engineering Department. He has been an Elite Applications-CAE Application Engineer with TEKYAZ Technological Software, Istanbul. His research interests include CAD, CAE, and CFD analysis.

OMER AKGUN received the Ph.D. degree in communication engineering from Yildiz Technical University, in 2009, and the Ph.D. degree from the Electronic and Communication Education Department, Marmara University, in 2011. He is currently an Assistant Professor with the Department of Computer Engineering, Technology Faculty, Marmara University. His current research interests include signal processing, biomedical signal processing, signal modeling, and communication systems.

TAHIR CETIN AKINCI (Senior Member, IEEE) received the B.S. degree in electrical engineering and the M.S. and Ph.D. degrees from Marmara University, Istanbul, Turkey, in 2005 and 2010, respectively. He was a Research Assistant with Marmara University, from 2003 to 2010. He was an Associate Professor with Istanbul Technical University (ITU), from 2016 to 2021. He has been a Full Professor with the Electrical Engineering Department, ITU, since 2021. He has also been a Visiting Scholar with the University of California at Riverside (UCR), since 2021. His research interests include data analytics, artificial neural networks, deep learning, machine learning, cognitive systems, signal processing, and data analysis.